

Electronic Supplementary Information

Support Facet Effects on the Performance of V_2O_5 - WO_3 - CeO_2/TiO_2 Catalysts for Selective Catalytic Reduction of NO with NH_3

Jianyou Liang^{a,b}, Haining Sun^c, Bolian Xu^a, Yubing Liu^{a,c,*}, Lei Yu^{d,*} and Yining Fan^{a,*}

^a *Key Laboratory of Mesoscopic Chemistry of MOE, Jiangsu Provincial Key Laboratory of Vehicle Emissions Control, Jiangsu Provincial Key Laboratory of Nanotechnology, School of Chemistry and Chemical Engineering, Nanjing University, Nanjing 210023, China*

^b *School of Chemical Engineering, Yangzhou Polytechnic Institute, Yangzhou 225127, China*

^c *Nanjing Institute of Microinterface Technology, Nanjing 210047, China*

^d *School of Chemistry and Materials, Yangzhou University, Yangzhou 225002, China*

^e *School of Environment and Safety Engineering, Nanjing Polytechnic Institute, Nanjing 210048, China*

**Corresponding Authors:*

E-mail: ybliu@nju.edu.cn (Y. Liu), yulei@yzu.edu.cn (L. Yu), ynfan@nju.edu.cn (Y. Fan)

Catalysts characterization

X-ray diffraction (XRD) patterns were acquired using a Shimadzu 6000 X-ray diffractometer equipped with Cu K α radiation ($\lambda = 1.5406 \text{ \AA}$). The measurements were performed at a tube voltage of 40 kV and a current of 30 mA. Data were collected over a 2θ range of 10° to 60° with a scanning rate of 5° min^{-1} and a step size of 0.04° .

The microstructure and morphology of the supports were examined by transmission electron microscopy (TEM) using a JEM-2100 instrument operated at an accelerating voltage of 200 kV. High-resolution TEM (HRTEM) imaging was conducted to resolve atomic lattice fringes, with the instrument possessing a point resolution of 0.23 nm and a line resolution of 0.14 nm.

Specific surface areas were determined via nitrogen physisorption at -196°C using a Micrometrics ASAP 2020 analyzer. Prior to analysis, approximately 0.15 g of each powder sample was degassed under a N_2/He mixture flow at 300°C for 6 h to remove adsorbed moisture and contaminants.

Raman spectra were obtained using a LabRAM Aramis spectrometer with an excitation wavelength of 633 nm. Each spectrum was obtained by accumulating 20 scans.

H_2 temperature-programmed reduction (H_2 -TPR) was conducted in a quartz U-tube reactor. 0.1 g of the catalyst was exposed to a 5 vol% H_2/Ar (20 mL min^{-1}) at a heating rate of $10^\circ\text{C min}^{-1}$. The H_2 consumption signal was recorded using a thermal conductivity detector (TCD).

NH_3 temperature-programmed desorption (NH_3 -TPD) was performed in a quartz U-tube reactor. 0.25 g of the catalyst was first pretreated in a helium flow at 400°C for 0.5 h, cooled to room temperature, and then saturated with liquid ammonia. The sample

was purged with helium (20 mL min^{-1}) for 0.5 h to remove physically adsorbed species. The temperature was ramped to $500 \text{ }^\circ\text{C}$ at $5 \text{ }^\circ\text{C min}^{-1}$. The desorbed NH_3 was detected by a TCD.

NH_3 temperature-programmed oxidation (NH_3 -TPO) was performed in a fix-bed quartz U-tube reactor. 0.2 g of the catalyst was pretreated in an argon flow at $400 \text{ }^\circ\text{C}$ for 0.5 h and then cooled to room temperature. The gas was switched to a mixture containing 2000 ppm NH_3 and 4 vol% O_2 balanced with Ar. The temperature was then increased from room temperature to $500 \text{ }^\circ\text{C}$ at a heating rate of $10 \text{ }^\circ\text{C min}^{-1}$. The outlet gases, including NO ($m/z=30$), NH_3 ($m/z = 17$), N_2O ($m/z = 44$) and N_2 ($m/z = 28$), were analyzed in real-time using a quadrupole mass spectrometer.

The *quasi in situ* XPS measurements were carried out on a PHI 5000 VersaProbe system with a monochromatic Al $K\alpha$ X-ray source (1486.6 eV , 25 W). Prior to analysis, the catalysts were subjected to the SCR reaction at $300 \text{ }^\circ\text{C}$ for 20 min in an attached reaction chamber. Subsequently, they were transferred under an inert atmosphere to an ultra-high vacuum (UHV) chamber ($< 5 \times 10^{-7} \text{ Pa}$) for outgassing. All binding energies were calibrated using contaminant carbon ($\text{C}1s = 284.6 \text{ eV}$) as a reference.

The *in situ* DRIFTS was performed on a Bruker Tensor II spectrometer equipped with a liquid nitrogen-cooled MCT detector. The catalyst powder was loaded into the Harrick IR cell and pretreated under an argon flow at $400 \text{ }^\circ\text{C}$ for 0.5 h to obtain a clean surface. Background spectra were collected at desired temperatures during cooling under argon and were subtracted from the corresponding sample spectra. All spectra were recorded by accumulating 64 scans at a resolution of 4 cm^{-1} . For NH_3 adsorption studies, the pretreated sample was cooled to room temperature and exposed to liquid NH_3 until saturation. After purging with argon for 1 h, spectra were collected at specific temperatures. To probe the reactivity of adsorbed ammonia species, the catalyst was

first saturated with NH_3 at 150 °C, purged with argon for 1 h, and then exposed to a flow of ($\text{NO} + \text{O}_2$) gas balanced with Ar. The temporal evolution of the IR bands corresponding to surface-adsorbed species was recorded.

Results and discussion

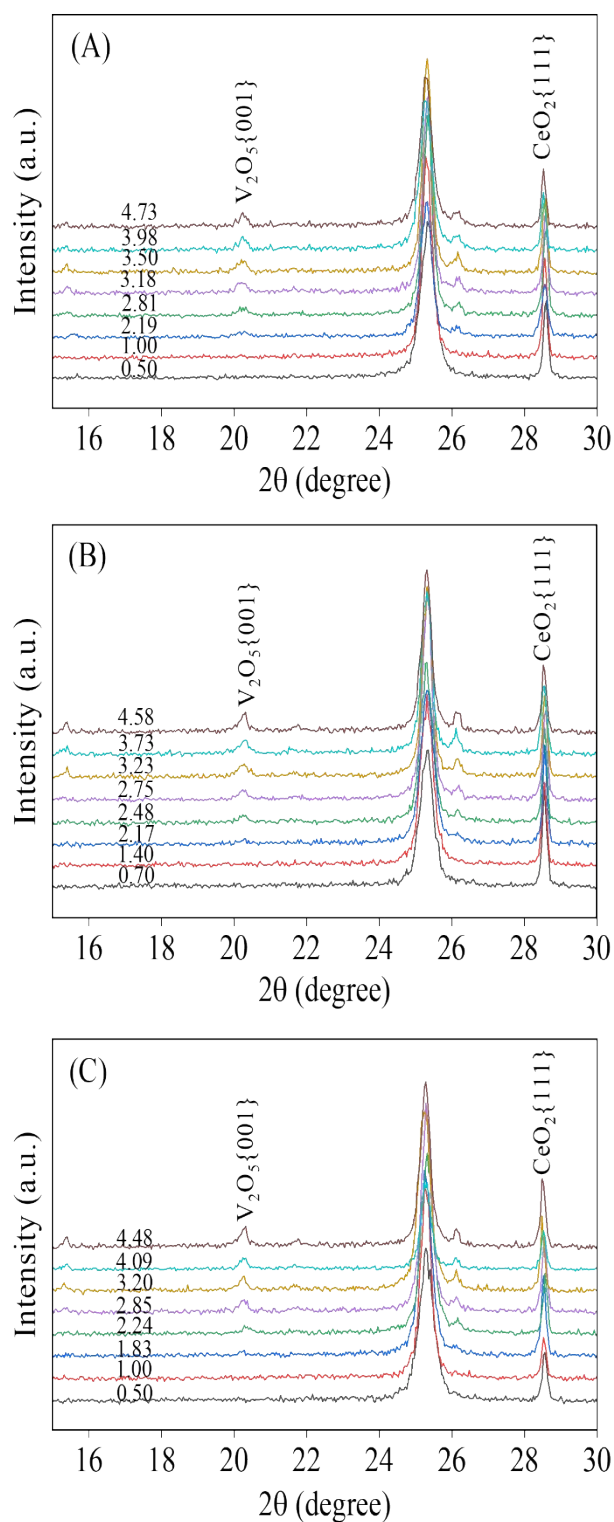


Fig. S1. XRD spectra of (A) V_2O_5/TiO_2 -NS{001}, (B) V_2O_5/TiO_2 -NP{101} and (C) V_2O_5/TiO_2 -NL{111} catalysts with different V_2O_5 loading amounts (mmol $VO_x/100$ m^2 TiO_2).

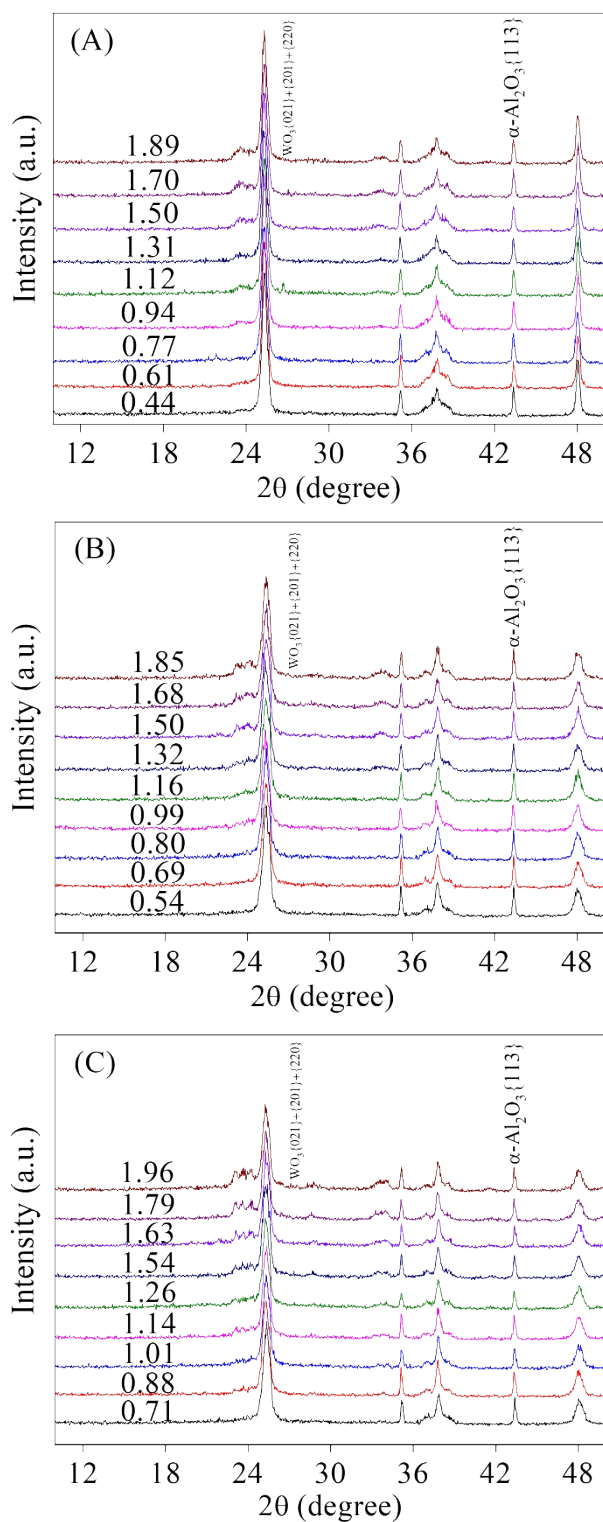


Fig. S2. XRD spectra of (A) WO₃/TiO₂-NS{001}, (B) WO₃/TiO₂-NP{101} and (C) WO₃/TiO₂-NL{111} samples with different WO₃ loading amounts (mmol WO_x/100 m² TiO₂).

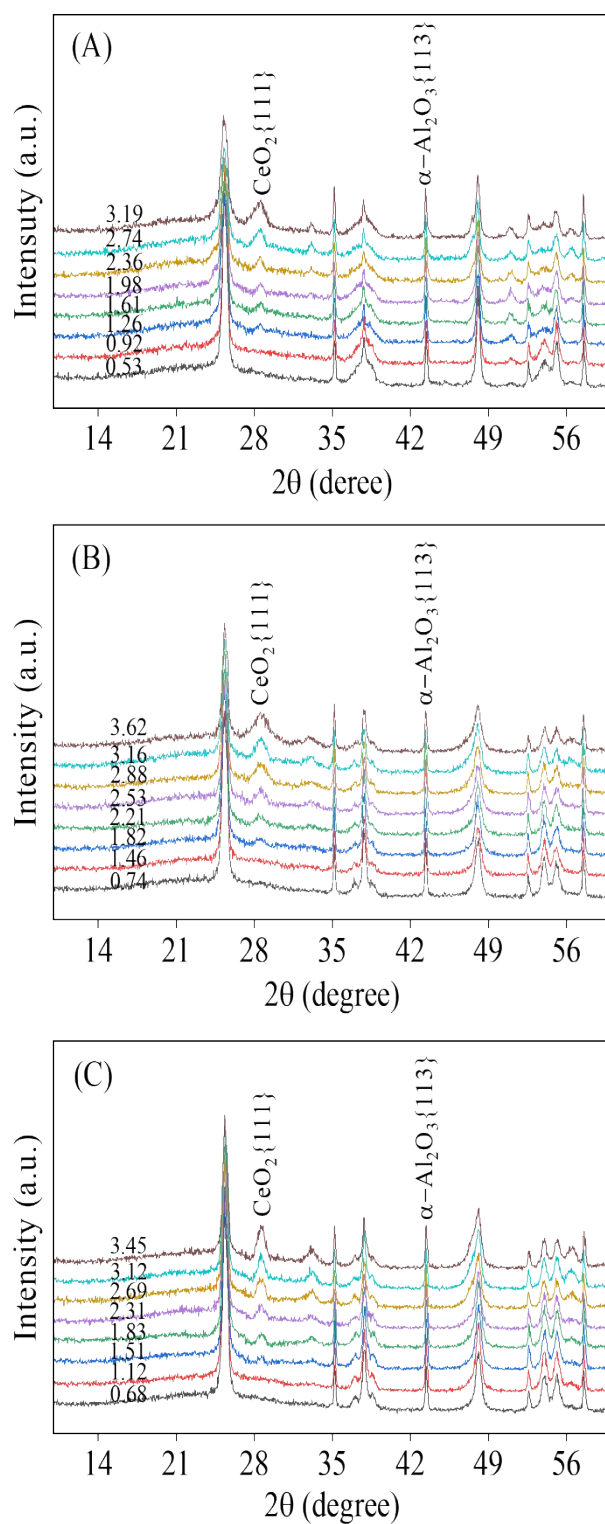


Fig. S3. XRD spectra of (A) CeO₂/TiO₂-NS{001}, (B) CeO₂/TiO₂-NP{101} and (C) CeO₂/TiO₂-NL{111} samples with different CeO₂ loading amounts (mmol CeO_x/100 m² TiO₂).

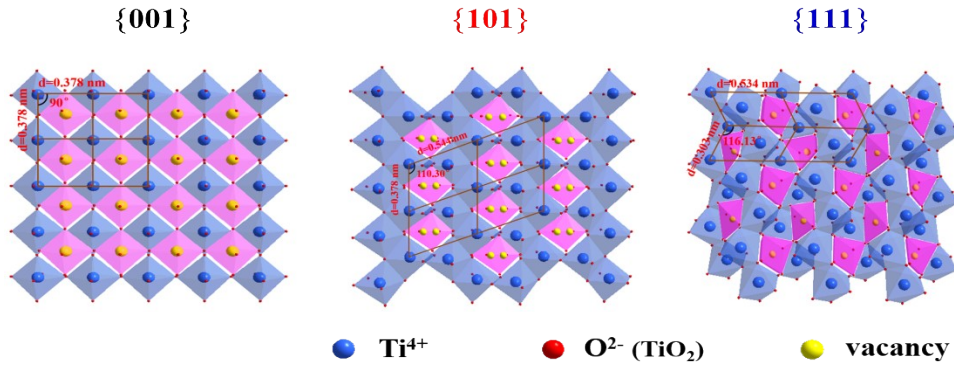


Fig. S4. Sizes of different facet structures of anatase TiO_2 supports.

The calculation of surface vacancy density of anatase TiO_2 supports

The vacancy sites without considering the exposed surface facet composition were calculated as follows:

Octahedral vacancy capacity for exposed $\text{TiO}_2\{001\}$ facet = 1 vacancy site/(0.378 nm \times 0.378 nm) = 6.92×10^{20} vacancy sites/100 m^2 = 1.1 mmol sites/100 m^2 TiO_2

Tetrahedral vacancy capacity for exposed $\text{TiO}_2\{101\}$ facet = 2 vacancy sites/(0.378 nm \times 0.544 nm \times $\sin 110.30^\circ$) = 10.3×10^{20} vacancy sites/100 m^2 = 1.7 mmol sites/100 m^2 TiO_2

Octahedral vacancy capacity for exposed $\text{TiO}_2\{111\}$ facet = 1 vacancy site/(0.303 nm \times 0.534 nm \times $\sin 116.13^\circ$) = 6.89×10^{20} vacancy sites/100 m^2 = 1.2 mmol sites/100 m^2 TiO_2

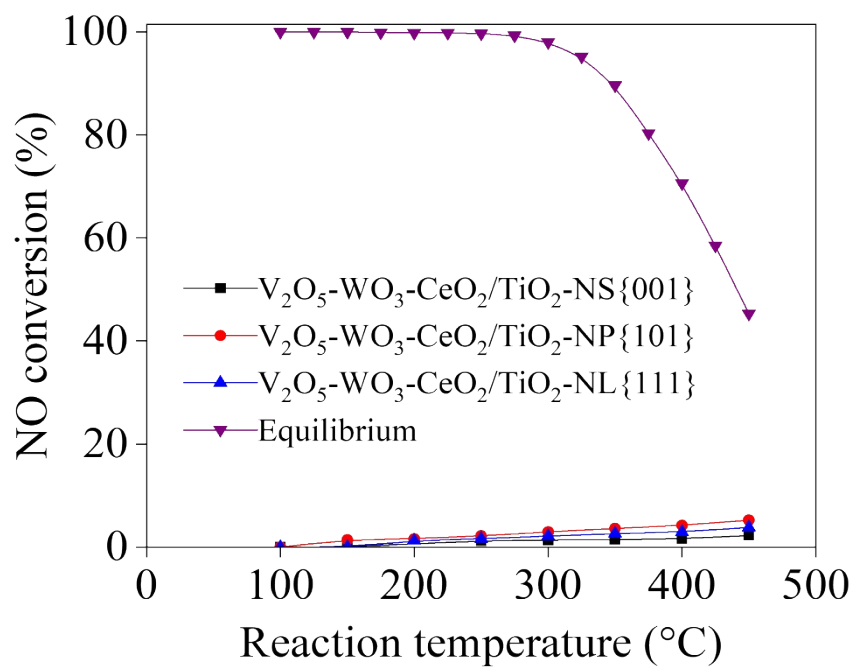


Fig. S5. Catalytic performance of supported $V_2O_5-WO_3-CeO_2/TiO_2$ catalysts for NO oxidation.

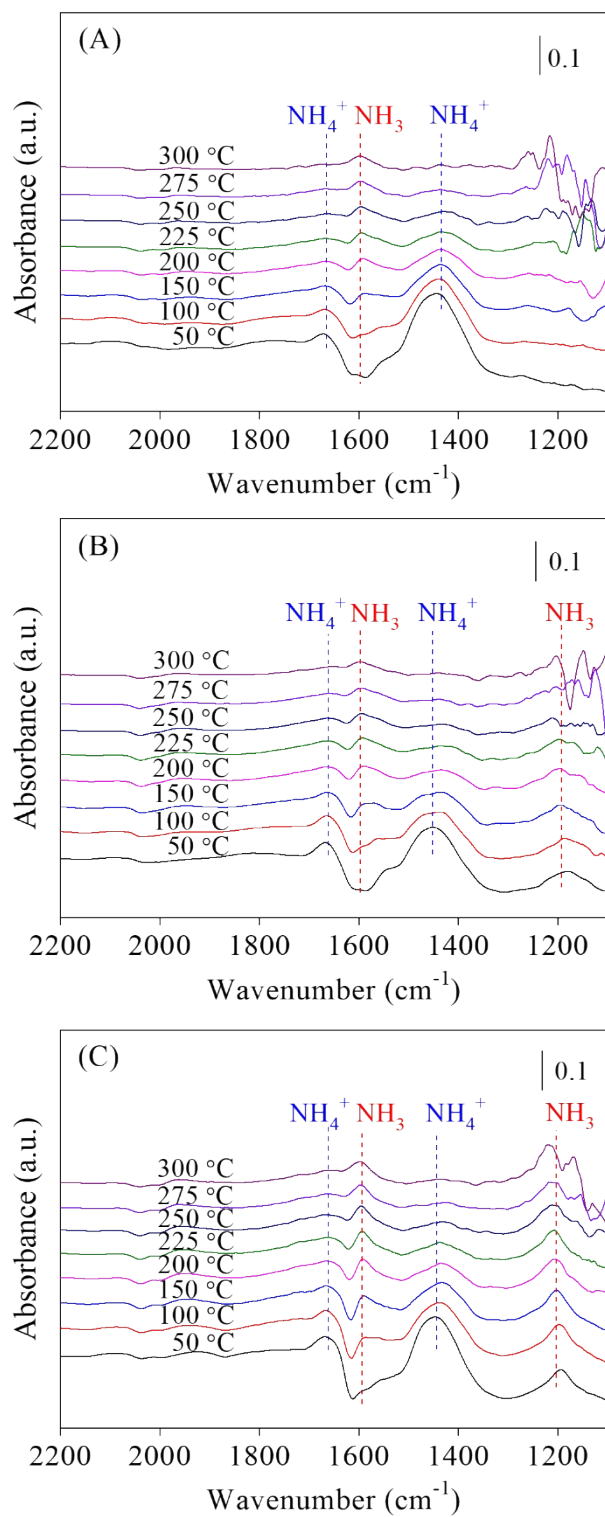


Fig. S6. NH_3 -IR spectra of (A) V_2O_5 - WO_3 - $\text{CeO}_2/\text{TiO}_2$ -NS{001}, (B) V_2O_5 - WO_3 - $\text{CeO}_2/\text{TiO}_2$ -NP{101} and (C) V_2O_5 - WO_3 - $\text{CeO}_2/\text{TiO}_2$ -NL{111} catalysts.

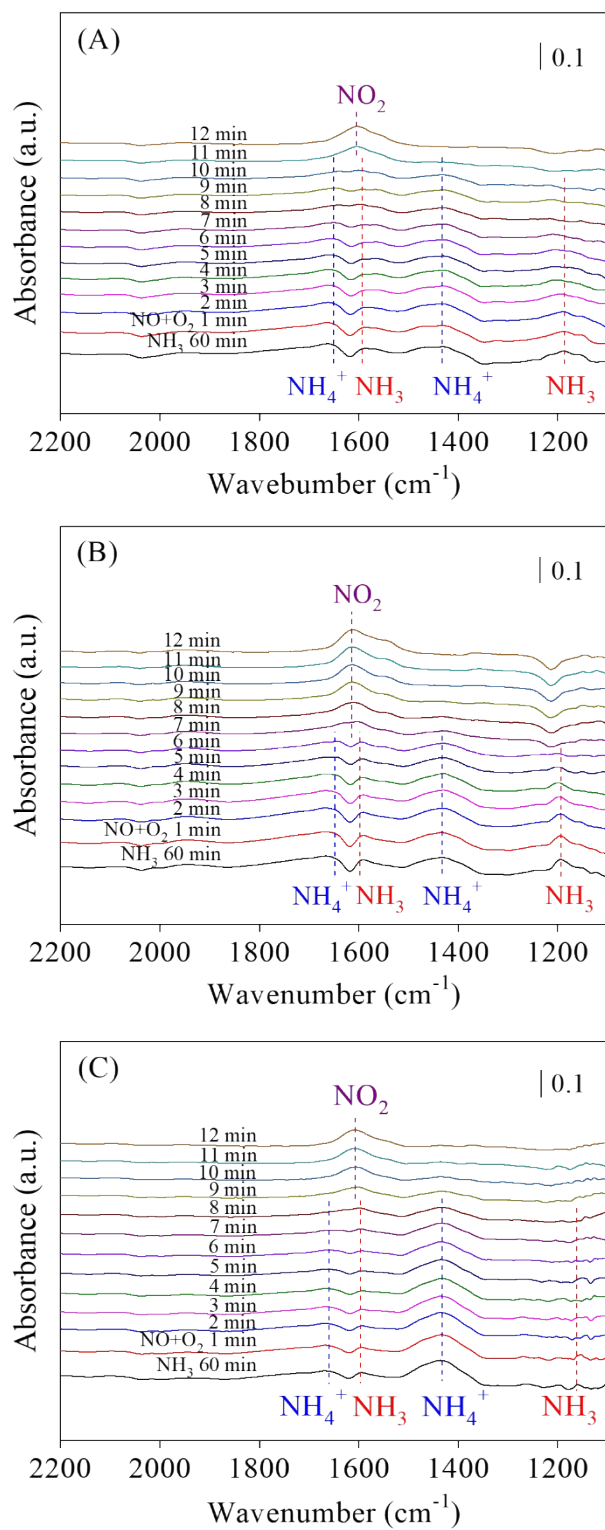


Fig. S7. Reactivity of pre-adsorption NH_3 -IR spectra of (A) $\text{V}_2\text{O}_5\text{-WO}_3\text{-CeO}_2/\text{TiO}_2\text{-NS}\{001\}$, (B) $\text{V}_2\text{O}_5\text{-WO}_3\text{-CeO}_2/\text{TiO}_2\text{-NP}\{101\}$ and (C) $\text{V}_2\text{O}_5\text{-WO}_3\text{-CeO}_2/\text{TiO}_2\text{-NL}\{111\}$ catalysts with $\text{NO} + \text{O}_2$ at $200\text{ }^\circ\text{C}$.